577677

Sandia National Laboratories

Operated for the United States Department of Energy
by National Technology and Engineering Solutions
of Sandia, LLC.

Albuquerque, New Mexico 87185-0101
Livermore, California 94551-0969

date: *July 21, 2022*

to: Sandia National Laboratory WIPP Records Center

from: Paul S. Domski, SNL WIPP Geochemistry *signature on file*

subject: EPA Issue 23: Implementation of the Neck et al. (2009) Am(III) Model

Introduction

In a letter from the EPA to DOE (Peake, 2018) the EPA summarized issues that the DOE had committed to resolving. Issue 23 regarding the WIPP Am(III) model (Peake, 2018), the EPA requested that the DOE update the WIPP Am(III) model using the model recommended in Neck et al. (2009), hereafter called the "Neck model". The current memorandum, provides verification of the updated Am(III) model compared to the Neck et al. (2009) experimental data, shows americium hydroxide solid phase stability diagrams in the presence of carbonate, and compares the results of using DATA0.FM5 on the CRA-2019 Deferred Performance Assessment (DPA) baseline actinide solubility model to that calculated with this updated Am(III) model using the Neck et al. (2009) parameters.

The Neck et al. (2009) Am(III) Experimental Data and Model

Neck et al. (2009) performed undersaturation experiments using $Nd(OH)_3(cr)$ synthesized in the lab from $Nd_2O_3(cr)$ in pure water under a $CO_2(g)$ free argon atmosphere. The $Nd_2O_3(cr)$, being unstable in the aqueous environment hydrated to a Nd – OH phase, and after a 3-month storage period was identified by X-ray diffraction (XRD) as crystalline $Nd(OH)_3(cr)$. This solid was used as the solubility controlling phase. Matrix solutions of NaCl (0.1, 0.5, 2.5, and 5.0 M), $MgCl_2$, and $CaCl_2$ (0.25, 1.0, 2.5, 3.5 M for Mg & Ca) were prepared using standard methods and the samples for solubility measurements were prepared and stored in an argon glove box at 22 ± 2 °C for equilibration times of 6 to 150 days. Ultrafiltration and ultracentrifugation techniques were used for phase separation and samples were analyzed for H^+ and Nd concentrations. The pH was measured with a "combination of pH electrodes (type ROSS, Orion)", and the Nd concentrations using "inductively coupled plasma-mass spectroscopy (ICP-MS) (ELAN 6100 Perkin Elmer); detection limit: 10^{-10} –10^{-9} M, depending on the concentration of the background electrolyte". See Neck et al. (2009) for details regarding the conversion of pH to pmH. The solids remaining in the experimental vessels were analyzed using XRD and scanning electron microscopy-energy-dispersive spectrometry (SEM-EDS) to determine if any phase transformations had occurred. The results of the solids characterization revealed that the solubility limiting phase, $Nd(OH)_3(cr)$, was unchanged for all matrix solutions with the exception of the 4.5 M $MgCl_2$ matrix solution where a neodymium hydroxy-chloride phase of lower solubility than $Nd(OH)_3(cr)$ was identified by the SEM-EDS. The results for the 4.5 $MgCl_2$ solution were not included in Neck et al. (2009).

WIPP:4.2.1.PA:QA-C:576427 Information Only

Neck et al. (2009) used their experimental data from the sodium, calcium, and magnesium chloride solutions to derive a log K value for $Nd(OH)_3(s)$ of 17.2 ± 0.4. Neck states that their derived value falls between that recommended by Baes and Mesmer (1976) of 18.66 ± 0.55 "*for fresh, amorphous precipitates of $Nd(OH)_3(s)$ and 16.02 ± 0.37 for aged and crystalline $Nd(OH)_3(s)$.*" Since crystalline $Nd(OH)_3(cr)$ was identified in the post-test solids analysis of Neck et al. (2009) it may be expected that the derived log K would reflect the higher crystallinity, however, the issue of Am-hydroxide crystallinity as it relates to solubility is not straightforward.

From Neck et al. (2009):

The use of the notation "crystalline" and "amorphous" to describe a solid phase and thereby its solubility is an oversimplification. The X-ray diffraction (XRD) data give only information of the bulk structure, while the solubility is determined by the surface characteristics or by fractions of smaller ("amorphous") particles included in a bulk crystalline solid.

This observation may explain why the Neck value of log K for $Nd(OH)_3(s)$ of 17.2 ± 0.4 is intermediate between the amorphous and crystalline values of the other authors.

The EPA specified in Issue 23 (Peake, 2018) that the DOE should include the Neck model for americium hydroxide ($Am(OH)_3(s)$) in the WIPP thermodynamic database. The DOE made the decision to construct a "one off" database, that is a database constructed from the current qualified database, DATA0.FM5 (Domski, 2020), that will be used to demonstrate how inclusion of the Neck et al. (2009) americium model affects solubility for WIPP relevant conditions. This database was not intended to be used for quality affecting work, in other words, it was not intended for recertification work. Neck et al. (2009) provides experimental data and parameters (log K values and Pitzer parameters), derived from their data, as well as recommended parameter values taken from the literature, most notably the Nuclear Energy Agency (NEA) volume of Guillamont et al. (2003) for the An(III) thermodynamic model.

Neck et al. (2009) provides two values for the log K for the amorphous An(III) – hydroxide phase, the first for $Am(OH)_3(am)$ from Guillamont et al. (2003) log K = 16.9 ±0.8, and the second derived from the $Nd(OH)_3(s)$[1] experimental solubility data contained in Neck et al. (2009), log K = 17.2 ±0.4. Likewise, for the crystalline/aged form of An(III) – hydroxide Neck et al. (2009) recommends the value of log K = 15.6 ±0.6 for $Am(OH)_3(cr/aged)$ from Guillamont et al. (2003), and log K = 16.0 ±0.4 for $Nd(OH)_3(cr/aged)$ from Diakonov et al. (1998). Accounting for the uncertainty, the log K values for each polymorph is essentially the same, and because they were derived for Am(III) and not Nd(III) the log K values for $Am(OH)_3(am)$ and $Am(OH)_3(cr/aged)$ of Guillamont et al. (2003) will be included in the WIPP database. This was also the recommendation of Neck et al. (2009).

Table 1 provides the reactions and additions, or changes, to log K and log β values that are included in the DATA0.NK5 database. Table 2 contains the Pitzer parameters included in the DATA0.NK5 database. Note that the Neck model does not include the Am(III) – carbonate system, the Am(III) – sulfate system, nor the Am(III) – Organic ligand systems (acetate, citrate, EDTA, and oxalate); therefore, these systems were retained from DATA0.FM5. Both the Neck model and the chemical

[1] The notation "$Nd(OH)_3$ (s)" is used by Neck because the exact nature of the crystallinity of the solubility controlling phase is uncertain. In the current memo "$Nd(OH)_3(s)$" will only be used in the context as defined by Neck, and "$Am(OH)_3(s)$" will be used specifically to define the Am – OH phase associated with log K = 14.49 (Giambalvo, 2002).

Information Only

systems retained from DATA0.FM5 are based on the Harvie et al. (1984) model, thus internal consistency was maintained.

Table 1. Equilibrium constants (log K values) and aqueous species stability constants (log β values) included in the WIPP Am(III) model, the DATA0.NK5 database.

Reaction	log K		Notes
	WIPP Model DATA0.FM5	Neck et al. (2009) DATA0.NK5	
Solid Phases			
$Am(OH)_3(am) + 3H^+ \rightleftharpoons Am^{3+} + 3H_2O$	NA	16.9 ± 0.8	Added to DATA0.NK5
$Am(OH)_3$(cr-aged) + $3H^+ \rightleftharpoons Am^{3+} + 3H_2O$	NA	15.6 ± 0.6	Added to DATA0.NK5
$Am(OH)_3(s) + 3H^+ \rightleftharpoons Am^{3+} + 3H_2O$	14.49	NA	Retained in DATA0.NK5
$AmOHCO_3(c)$[2] $+ 2H^+ \rightleftharpoons Am^{3+} + H_2O + HCO_3^-$	1.64	NA	Retained in DATA0.NK5
$NaAm(CO_3)_2 \cdot 6H_2O(s) + 2H^+ \rightleftharpoons Na^+ + Am^{3+} + 2HCO_3^- + 6H_2O$	-0.71	NA	Retained in DATA0.NK5
Aqueous Species			
$AmCO_3^+ + H^+ \rightleftharpoons Am^{3+} + HCO_3^-$	2.24	NA	Retained in DATA0.NK5
$Am(CO_3)_2^- + 2H^+ \rightleftharpoons Am^{3+} + 2HCO_3^-$	7.68	NA	Retained in DATA0.NK5
$Am(CO_3)_3^{3-} + 3H^+ \rightleftharpoons Am^{3+} + 3HCO_3^-$	15.8	NA	Retained in DATA0.NK5
$Am(CO_3)_4^{5-} + 4H^+ \rightleftharpoons Am^{3+} + 4HCO_3^-$	28.4	NA	Retained in DATA0.NK5
$Am(OH)^{2+} + H^+ \rightleftharpoons Am^{3+} + H_2O$	7.56	7.2 ± 0.5	Log β updated
$Am(OH)_2^+ + 2H^+ \rightleftharpoons Am^{3+} + 2H_2O$	15.7	15.1 ± 0.7	Log β updated
$Am(OH)_3(aq) + 3H^+ \rightleftharpoons Am^{3+} + 3H_2O$	25.7	26.2 ± 0.5	Log β updated
$Am(OH)_4^- + 4H^+ \rightleftharpoons Am^{3+} + 4H_2O$	NA	40.7 ± 0.7	Added to DATA0.NK5
$AmCl^{2+} \rightleftharpoons Am^{3+} + Cl^-$	-0.24	-0.24 ± 0.03	Log β same as WIPP model
$AmCl_2^+ \rightleftharpoons Am^{3+} + 2Cl^-$	0.74	0.74 ± 0.05	Log β same as WIPP model
$AmSO_4^+ \rightleftharpoons Am^{3+} + SO_4^{2-}$	-3.25	NA	Retained in DATA0.NK5
$Am(SO_4)_2^- \rightleftharpoons Am^{3+} + 2SO_4^{2-}$	-3.70	NA	Retained in DATA0.NK5
$AmAcetate^{2+} \rightleftharpoons Am^{3+} + Acetate^-$	-2.74	NA	Retained in DATA0.NK5
$AmCitrate(aq) \rightleftharpoons Am^{3+} + Citrate^{3-}$	-8.80	NA	Retained in DATA0.NK5
$AmEDTA^- \rightleftharpoons Am^{3+} + EDTA^{4-}$	-18.97	NA	Retained in DATA0.NK5
$AmLactate^{2+} \rightleftharpoons Am^{3+} + Lactate^-$	-3.71	NA	Retained in DATA0.NK5

[2] Felmy et al. (1990) identified the crystalline form of $AmOHCO_3$ as the solubility controlling phase in systems with total carbonate (TIC) <0.1 M and pH between 5.5 and 13.1 over short time frames of 36 to 66 days.

Information Only

Reaction	log K		Notes
	WIPP Model DATA0.FM5	Neck et al. (2009) DATA0.NK5	
$AmOxalate^{+} \rightleftharpoons Am^{3+} + Oxalate^{2-}$	-6.16	NA	Retained in DATA0.NK5
$Ca[Am(OH)_3]^{2+} + 3H^{+} \rightleftharpoons Am^{3+} + Ca^{2+} + 3H_2O$	NA	26.3 ± 0.5	Added to DATA0.NK5
$Ca_2[Am(OH)_4]^{3+} + 4H^{+} \rightleftharpoons Am^{3+} + 2Ca^{2+} + 4H_2O$	NA	37.2 ± 0.6	Added to DATA0.NK5
$Ca_3[Am(OH)_6]^{3+} + 6H^{+} \rightleftharpoons Am^{3+} + 3Ca^{2+} + 6H_2O$	NA	60.7 ± 0.5	Added to DATA0.NK5

Table 2. The Pitzer interaction parameters included in the WIPP Am(III) model with the Neck et al. (2009) updated values.

I	J	$\beta^{(0)}$	$\beta^{(1)}$	$\beta^{(2)}$	C^{φ}	Source
Cation-Anion Interactions						
Am^{3+}	Cl^{-}	0.586	5.6	0	-0.016	Fanghänel and Kim (1998)[3]
Am^{3+}	SO_4^{2-}	1.79	15.0	0	0.6	Fanghänel and Kim (1998)[4]
Am^{3+}	ClO_4^{-}	0.8	5.35	0	-0.0048	Felmy et al. (1990)[2]
$Ca[Am(OH)_3]^{2+}$	Cl^{-}	0.21	1.6	0	0	Neck et al. (2009)[5]
$Ca_2[Am(OH)_4]^{3+}$	Cl^{-}	0.70	4.3	0	0	Neck et al. (2009)[3]
$Ca_3[Am(OH)_6]^{3+}$	Cl^{-}	0.37	4.3	0	0	Neck et al. (2009)[3]
$Am(CO_3)_3^{3-}$	Na^{+}	0.125	4.73	0	0.0007	Fanghänel et al. (1999)[2]
$Am(CO_3)_4^{5-}$	K^{+}	2.02	19.2	0	-0.305	Fanghänel and Kim (1998)[2]
$Am(CO_3)_4^{5-}$	Na^{+}	2.02	19.2	0	-0.305	Fanghänel and Kim (1998)[2]
$AmCO_3^{+}$	Cl^{-}	-0.072	0.403	0	0.0388	Fanghänel and Kim (1998)[2]
$Am(SO_4)_2^{-}$	K^{+}	-0.354	0.4	0	0.051	Fanghänel and Kim (1998)[2]
$Am(SO_4)_2^{-}$	Na^{+}	-0.354	0.4	0	0.051	Fanghänel and Kim (1998)[2]
$AmSO_4^{+}$	Cl^{-}	-0.091	-0.39	0	0.048	Fanghänel and Kim (1998)[2]
$AmCl^{2+}$	Cl^{-}	0.593	3.15	0	-0.006	Fanghänel and Kim (1998)[2]
$AmCl_2^{+}$	Cl^{-}	0.516	1.75	0	0.01	Fanghänel and Kim (1998)[2]

[3] Same value in both DATA0.FM5 and Neck et al. (2009)
[4] Sulfate, perchlorate, carbonate, and organic systems are not included in Neck et al. (2009), retained from DATA0.FM5
[5] New value from Neck et al. (2009)

Information Only

I	J	$\beta^{(0)}$	$\beta^{(1)}$	$\beta^{(2)}$	C^{φ}		Source
$AmOH^{2+}$	Cl^-	0.055	1.81	0	0		Neck et al. (2009)[3]
$Am(OH)_2^+$	Cl-	-0.13	0	0	0		Neck et al. (2009)[3]
$Am(OH)_4^-$	K^+/Na^+ Ca^{2+}/Mg^{2+}	0	0	0	0		Neck et al. (2009)[3]
$AmEDTA^-$	K^+	-0.224	0.29	0	0.002		Choppin et al. (2001)[2]
$AmLactate^{2+}$	Cl^-	0.840	1.74	0	-0.332		Moore et al. (1999)[2]
$AmAcetate^{2+}$	Cl^-	0.309	1.74	0	-0.132		Giambalvo (2002)[2]
$AmOxalate^+$	Cl^-	-0.937	0.29	0	0.248		Choppin et al. (2001)[2]
$AmEDTA^-$	Na^+	-0.224	0.29	0	0.002		Choppin et al. (2001)[2]

i	j	k	θ_{ij}	Ψ_{ijk}	λ_{ik}	Source
M^{3+}	Na^+	Cl^-	0.10	0	-	Könnecke et al (1997)[2]
	Ca^{2+}/Mg^{2+}	Cl^-	0.20	0	-	Könnecke et al (1997)[2]
MCl^{2+}	Na^+	Cl^-	0	0	-	Könnecke et al (1997)[2]
	Ca^{2+}/Mg^{2+}	Cl^-	-0.014	0	-	Könnecke et al (1997)[2]
MCl_2^+	Na^+	Cl^-	0	0	-	Könnecke et al (1997)[2]
	Ca^{2+}/Mg^{2+}	Cl^-	-0.196	0	-	Könnecke et al (1997)[2]
$M(OH)^{2+}$	Na^+	Cl^-	0	0	-	Neck et al. (2009)[3]
	Ca^{2+}/Mg^{2+}	Cl^-	0	0.04	-	Neck et al. (2009)[3]
$M(OH)_2^+$	Na^+	Cl^-	0	0	-	Neck et al. (2009)[3]
	Ca^{2+}/Mg^{2+}	Cl^-	0.29	0.07	-	Neck et al. (2009)[3]
$M(OH)_4^-$	Cl^-/OH^-	Na^+/K^+	0	0	-	Neck et al. (2009)[3]
	Cl^-	Ca^{2+}/Mg^{2+}	0	0	-	Neck et al. (2009)[3]
$M(OH)_3(aq)$	-	Na^+	-	-	-0.2	Neck et al. (2009)[3]
	-	K+	-	-	0	Neck et al. (2009)[3]
	-	Ca^{2+}/Mg^{2+}	-	-	0	Neck et al. (2009)[3]
	-	Cl^-/OH^-	-	-	0	Neck et al. (2009)[3]
$Ca[Am(OH)_3]^{2+}$	Ca^{2+}	Cl^-	0	0	-	Neck et al. (2009)[3]
$Ca_2[Am(OH)_4]^{3+}$	Ca^{2+}	Cl^-	0	0	-	Neck et al. (2009)[3]
$Ca_3[Am(OH)_6]^{3+}$	Ca^{2+}	Cl^-	0	0	-	Neck et al. (2009)[3]

Pitzer coefficients for M(III) species, where M = Am, Cm, Pu, and Nd.

The database DATA0.NK5 is archived in the zip file *Neck_An(III)_Model.zip*, which is stored at /nfs/data/CVSLIB/WIPP_EXTERNAL/ap153".

The Neck Model Compared to the Experimental Data

The Neck model as implemented in the EQ3/6 database DATA0.NK5 was compared to the measured neodymium solubility data presented in Neck et al. (2009) using the EQ3NR code to simulate Neck's solubility experiments. For each simulation the salt concentration of the matrix solution was used as input and the pmH was incremented at fixed values between the minimum and maximum experimental

Information Only

value(s) while the Am(III) concentration was calculated based on the equilibrium solubility of $Am(OH)_3$(am) and $Am(OH)_3$(cr-aged) for each salt concentration and pmH value.

The results of the validation exercise are shown in Figure 1 for sodium chloride matrix solutions, and Figure 2 for magnesium and calcium chloride matrix solutions. For the three matrix solutions at all concentrations and all pmH values the simulated solubility of the amorphous Am-hydroxide phases fits the experimental data better than the crystalline-aged Am-hydroxide phase. Figures 1 and 2 correspond to Figures 3 and 4 in Neck et al. (2009), respectively. Simulated (model) responses appear slightly different due to differences in the modeling software and the log K values of the solid phases, Am(III) hydroxide phases for the current work, and Nd(III) hydroxide for Neck et al. (2009).

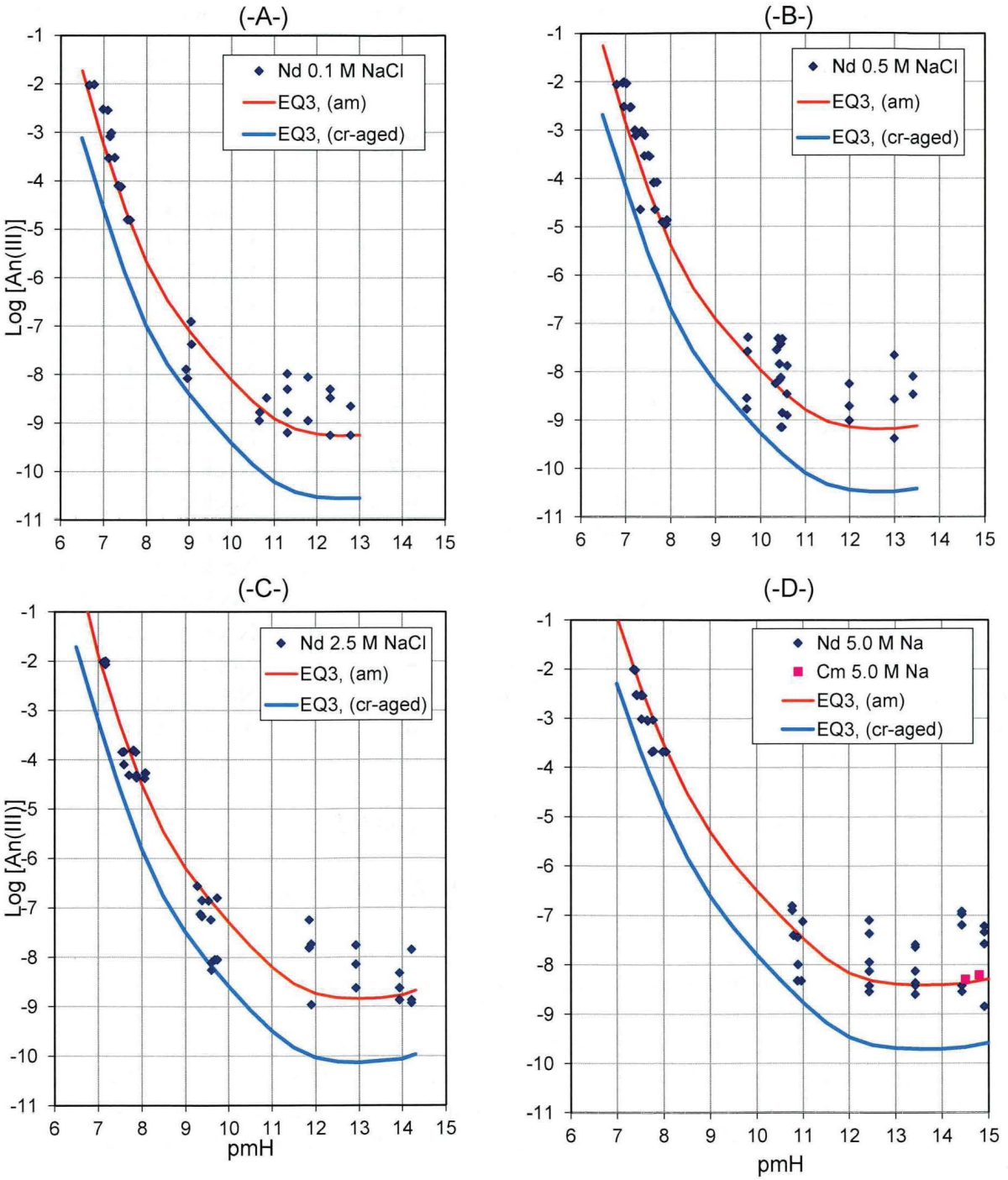

Information Only

Figure 1. Neck et al. (2009) An(III) model compared to $Nd(OH)_3(s)$ solubility data in NaCl matrix solution.

Information Only

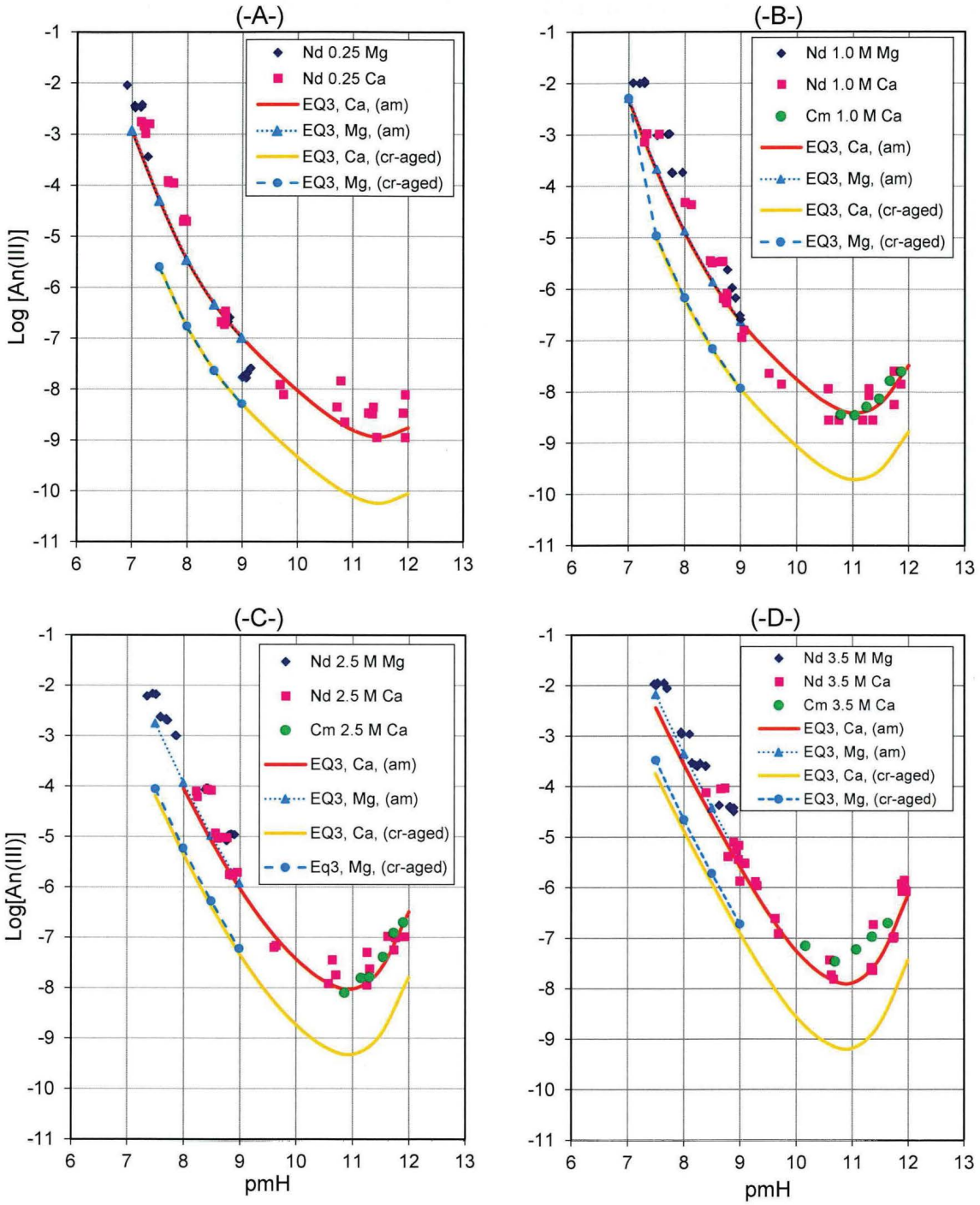

Figure 2. Neck et al. (2009) An(III) model compared to $Nd(OH)_3(s)$ solubility data in $MgCl_2$ and $CaCl_2$ matrix solutions.

The EQ3NR input/output files and the spreadsheet *Neck_Nd-data_Verification.xlsx* are archived in the zip file *Neck_An(III)_Model.zip*, which is stored at /nfs/data/CVSLIB/WIPP_EXTERNAL/ap153".

Information Only

Stability Fields of Am(III) Solids for WIPP Conditions

Neck et al. (2009) investigated the solubility of Nd – hydroxide in the Ca^{2+} – Mg^{2+} – Na^{+} – Cl^{-} – H_2O system(s), where the only anion species were OH^{-} and Cl^{-}. For the purposes of WIPP geochemistry we need to investigate the effect of other anion species, most notably, carbonate. The WIPP geochemistry model also includes sulfate and bromide, however, neither of those species form low-solubility phases, or high concentration aqueous species for expected WIPP conditions with Am(III) thereby removing them from consideration.

Neck et al. (2009) states:

> *"In the absence of carbonate, silicate, or phosphate, the solubility limiting solid phase is the An(III) hydroxide: $Am(OH)_3(s) + 3H^{+} \rightleftharpoons Am^{3+} + 3H_2O$".*

The WIPP actinide solubility model does not currently include silica or phosphate, it does, however, include carbonate. Therefore, the stability field of the Am(III) hydroxide and carbonate solids must be investigated for expected WIPP conditions. The WIPP conditions can be expressed in terms of the activity of water and the fugacity of carbon dioxide, conditions predicted by the WIPP baseline solubility model, and these two variables can be used to determine the stability fields of the Am(III) hydroxide and carbonate phases.

Table 3. The important reactions that define this system.

Eqn	Reaction	Log K		
1	$Am(OH)_3(x) + 3H^{+} \rightleftharpoons Am^{3+} + 3H_2O$	**(am)**	**(cr-aged)**	**(s)**
	Where x = am, cr-aged, or s	16.9	15.6	14.49
2	$AmOHCO_3(c) + 2H^{+} \rightleftharpoons Am^{3+} + H_2O + HCO_3^{-}$	1.64		
3	$CO_2(g) + H_2O \rightleftharpoons H^{+} + HCO_3^{-}$	-7.82		
Rearranging and Combining equations 1,2, and 3 gives the equilibrium conversion of $Am(OH)_3(x)$ to $AmOHCO_3(c)$:				
4	$Am(OH)_3(x) + CO_2(g) \rightleftharpoons AmOHCO_3(c) + H_2O$	**$\text{Log K}_{\text{conversion}}$ = Log K(x) + (-1.64) + (-7.82)**		
By convention the activity of pure solid phases is zero, therefore, the log K for equation 4 is the activity of the products divided by the activity of the reactants, or equation 5, as expressed in the $\log_{10}$ form.				
5	$\text{Log K}_{\text{conversion}} = \text{Log } \{H_2O\} - \text{Log } f_{CO2(g)}$			
6	$\text{Log } \{H_2O\} - \text{Log } f_{CO2(g)} = (\text{Log K(x)} + (-1.64) + (-7.82))$			
7	$\text{Log } f_{CO2(g)} = \text{Log } \{H_2O\} - (\text{Log K(x)} + (-1.64) + (-7.82))$			

Applying equation 7 from Table 3 the fugacity of $CO_2(g)$ may be calculated over a range of water activities for each Am – hydroxide phase which provides the stability field of the $Am(OH)_3(x)$ relative to $AmOHCO_3(c)$. The stability of the Am-hydroxide phases and $AmOHCO_3(c)$ were calculated in the Excel spreadsheet, *Stability_Am(OH)3(x)_AmOHCO3(s).xlsx*, and the results are plotted in Figure 3.

The WIPP conditions as represented in Figure 3 are the activity of water (a_{H2O}), 0.73, and $fCO_2(g)$, 2.02E-06, for ERDA-6 and GWB brines equilibrated with the Salado minerals (halite and anhydrite), the engineered barrier (brucite and hydromagnesite), the waste container and shielding materials (iron and lead), the organic ligands (acetate, citrate, EDTA, and oxalate), and the actinide solubility controlling phases (Tables 6 and 7, Domski and Sisk-Scott, 2019). The WIPP condition, plotted as a red square in Figure 3, is the final equilibrium state of the system, the state which determines the actinide solubilities, and where the brucite – hydromagnesite buffer invariant point controls the carbonate system.

Information Only

The stability fields of the three Am(III) hydroxide phases relative to $AmOHCO_3(c)$ are displayed in Figure 3 where the carbonate phase is stable above the line and the hydroxide phase is stable below the line, with the predicted WIPP fugacity of $CO_2(g)$ and activity of water is plotted as the single red square.

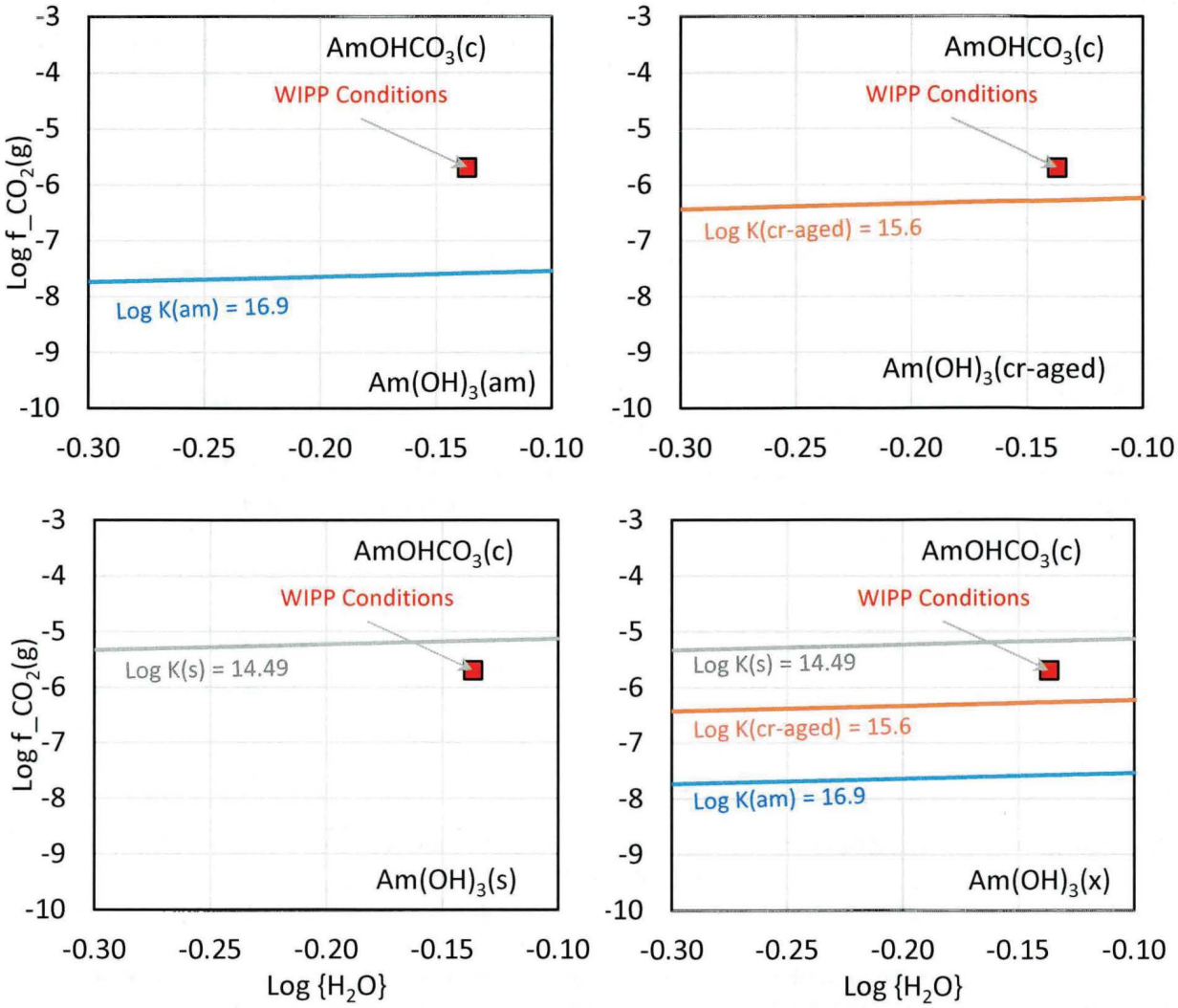

Figure 3. Stability field of the Am(III) hydroxide phases relative to $AmOHCO_3(c)$ for the WIPP predicted fugacity of $CO_2(g)$ and activity of water.

Figure 3 shows that for the predicted WIPP chemical conditions (a_{H2O} and $fCO_2(g)$) the solubility-controlling Am(III) phase is either $Am(OH)_3(s)$ or $AmOHCO_3(c)$. If $Am(OH)_3(s)$ is allowed to form in the modeled system, then it would be the solubility controlling phase for Am(III). However, if $Am(OH)_3(s)$ is not allowed to form in the modeled system, then $AmOHCO_3(c)$ becomes the Am(III) solubility controlling phase. For the predicted WIPP conditions the more soluble Am(III) hydroxides (am and cr-aged) are not stable and will not be the Am(III) solubility controlling phase.

The spreadsheet *Stability_Am(OH)3(x)_AmOHCO3(s).xlsx* is archived in the zip file *Neck_An(III)_Model.zip*, which is stored at "/nfs/data/CVSLIB/WIPP_EXTERNAL/ap153".

Information Only

Application of the Neck Model to the CRA-2019 Baseline Solubility Model

The CRA-2019 DPA minimum volume case of the baseline actinide solubility model for the ERDA-6 and GWB brines were run with DATA0.NK5, the database updated with the Neck model and compared to the results obtained using DATA0.FM5. The database, DATA0.FM5, was not used for CRA-2019 DPA (Domski and Sisk-Scott, 2019) rather DATA0.FM4 was used, therefore, there are slight differences in the results of Domski and Sisk-Scott (2019) with those documented herein. DATA0.FM5 was issued to correct minor transcription errors found in DATA0.FM4 documented in Domski (2020).

The actinide baseline solubility model is a two-step model:

Step 1. **Initial Solutions:** EQ3NR is used to equilibrate and speciate the brine compositions (ERDA-6 & GWB) with the inventory scaled masses of the organic ligands (acetate, oxalate, citrate, and EDTA) and the actinide concentrations are set via equilibrium with solubility controlling phases ($Am(OH)_3(x)$[6], $ThO_2(am)$, and $KNpO_2CO_3$). The conditions of low pH and high carbonate concentration of the initial solution ensures that an excess mass of actinides dissolve in this step. These dissolved concentrations are then passed to Step 2 and are subject to the evolving chemical environment of the reacting solution and where the stable solubility controlling phase may form.

Step 2. **Final Equilibrium System:** Using EQ6 the initial solution compositions from Step1 are reacted with the inventory-scaled masses of the engineered MgO barrier (represented as 50% brucite and 50% hydromagnesite), the iron and lead reactants representing the waste containers and radiation shielding, and the Salado Formation minerals halite and anhydrite. The model includes the effects of mineral phase dissolution and precipitation and organic ligand complexation. The model provides the actinide solubilities and the expected repository conditions. The expected repository conditions include the equilibrium pH, $fCO_2(g)$, activity of water, total inorganic carbon, ionic strength, the concentration of all dissolved constituents, and the solid phase budget.

The results of the model runs are listed in Tables 4 (GWB) and 5 (ERDA-6). Column 1, in Tables 4 and 5, used the DATA0.FM5 database, columns 2 through 4 were calculated using DATA0.NK5. In Step 1 of the EQ3/6 calculations the solubility controlling phase for each column was set as follows: Column 1 - $Am(OH)_3(s)$; Column 2 - $Am(OH)_3(am)$; Column 3 - $Am(OH)_3$(cr-aged); and Column 4 – no phase specified, with initial Am(III) concentration set to the CRA-2019 at inventory value.

Table 4. Baseline solubility model results for GWB using the CRA-2019 DPA inputs.

Column	1	2	3	4
Database	DATA0.FM5	DATA0.NK5	DATA0.NK5	DATA0.NK5
Filename	gwb_1x.6o	gwb_am.6o	gwb_cr.6o	gwb_in.6o[A]
Suppressed $Am(OH)_3(x)$[B] Phase(s)	none	(s) (cr-aged)	(s)	(s)
Pitzer pH	8.82	8.82	8.82	8.82
pcH	9.54	9.54	9.54	9.54
a(w)	0.73	0.73	0.73	0.73
(I)	7.56	7.56	7.56	7.56
Mass Solvent (kg)	0.61	0.61	0.61	0.61
Molality/molarity (L/kg.H_2O)	1.16	1.16	1.16	1.16
Am (m)	1.92E-07	1.12E-07	1.12E-07	1.12E-07
B (m)	2.60E-01	2.60E-01	2.60E-01	2.60E-01
Br (m)	4.37E-02	4.37E-02	4.37E-02	4.37E-02
Ca (m)	1.26E-02	1.26E-02	1.26E-02	1.26E-02

[6] $Am(OH)_3(x)$ x = am, cr-aged, or s.

Information Only

Column	1	2	3	4
Database	DATA0.FM5	DATA0.NK5	DATA0.NK5	DATA0.NK5
Filename	gwb_1x.6o	gwb_am.6o	gwb_cr.6o	gwb_in.6o[A]
Suppressed $Am(OH)_3(x)$[B] Phase(s)	none	(s) (cr-aged)	(s)	(s)
Cl (m)	6.26	6.26	6.26	6.26
Fe (m)	3.03E-05	3.03E-05	3.03E-05	3.03E-05
K (m)	7.67E-01	7.67E-01	7.67E-01	7.67E-01
Mg (m)	4.03E-01	4.03E-01	4.03E-01	4.03E-01
Na (m)	5.44	5.44	5.44	5.44
Np (m)	4.66E-07	4.66E-07	4.66E-07	4.66E-07
Pb (m)	2.20E-02	2.20E-02	2.20E-02	2.20E-02
S (m)	2.68E-01	2.68E-01	2.68E-01	2.68E-01
Th (m)	6.31E-08	6.31E-08	6.31E-08	6.31E-08
Acetate (m)	4.65E-02	4.65E-02	4.65E-02	4.65E-02
Citrate (m)	3.78E-03	3.78E-03	3.78E-03	3.78E-03
EDTA (m)	1.30E-04	1.30E-04	1.30E-04	1.30E-04
Oxalate (m)	3.79E-04	3.79E-04	3.79E-04	3.79E-04
TIC (m)	2.89E-04	2.89E-04	2.89E-04	2.89E-04
$CO_2(g)$ Fugacity	2.02E-06	2.02E-06	2.02E-06	2.02E-06
Solid Phase	Saturation Index (SI)			
$Am(OH)_3(am)$	[C]	-1.89	-1.89	-1.89
$Am(OH)_3$(cr-aged)	[C]	-0.59	-0.59	-0.59
$Am(OH)_3(s)$	0.00	0.52	0.52	0.52
$AmOHCO_3(c)$	-0.52	0.00	0.00	0.00

A - The scaled inventory mass of the total emplaced Am(III) at repository closure in 2033 using the 2018-PAIR data (VanSoest, 2018) was used to set the initial Am(III) concentration in Step 1. See APPENDIX A for calculation of the total Am(III).
B - $Am(OH)_3(x)$ x = am, cr-aged, or s.
C - $Am(OH)_3$(am) and $Am(OH)_3$(cr-aged) are not included in DATA0.FM5

Table 5. Baseline solubility model results for ERDA-6 using the CRA-2019 DPA inputs.

Column	1	2	3	4
Database	DATA0.FM5	DATA0.NK5	DATA0.NK5	DATA0.NK5
Filename	erda_1x.6o	erda_am.6o	erda_cr.6o	erda_in.6o[A]
Suppressed $Am(OH)_3(x)$[B] Phase(s)	none	(s) (cr-aged)	(s)	(s)
Pitzer pH	8.79	8.81	8.80	8.79
pcH	9.57	9.53	9.56	9.57
a(w)	0.73	0.73	0.73	0.73
(I)	7.43	7.46	7.43	7.43
Mass Solvent (kg)	0.166	0.169	0.167	0.166
Molality/molarity (L/kg.H_2O)	1.16	1.16	1.16	1.16
Am (m)	3.27E-07	2.92E-07	2.89E-07	2.92E-07
B (m)	2.81E-01	3.10E-01	2.89E-01	2.81E-01
Br (m)	6.63E-02	6.51E-02	6.57E-02	6.63E-02
Ca (m)	1.14E-02	1.36E-02	1.20E-02	1.14E-02
Cl (m)	6.60	6.22	6.49	6.61
Fe (m)	2.77E-05	2.98E-05	2.83E-05	2.77E-05
K (m)	5.85E-01	5.74E-01	5.79E-01	5.85E-01
Mg (m)	3.68E-01	4.56E-01	3.91E-01	3.67E-01
Na (m)	5.12	5.32	5.18	5.12
Np (m)	1.55E-06	1.45E-06	1.52E-06	1.55E-06
Pb (m)	2.03E-02	2.13E-02	2.06E-02	2.03E-02
S (m)	2.74E-01	2.64E-01	2.71E-01	2.74E-01
Th (m)	6.22E-08	6.27E-08	6.23E-08	6.22E-08
Acetate (m)	1.71E-01	1.68E-01	1.69E-01	1.71E-01

Information Only

Column	1	2	3	4
Database	**DATA0.FM5**	**DATA0.NK5**	**DATA0.NK5**	**DATA0.NK5**
Filename	**erda_1x.6o**	**erda_am.6o**	**erda_cr.6o**	**erda_in.6o[A]**
Suppressed $Am(OH)_3(x)$[B] Phase(s)	**none**	**(s) (cr-aged)**	**(s)**	**(s)**
Citrate (m)	1.39E-02	1.36E-02	1.37E-02	1.39E-02
EDTA (m)	4.77E-04	4.69E-04	4.73E-04	4.78E-04
Oxalate (m)	3.81E-04	3.86E-04	3.82E-04	3.81E-04
TIC (m)	2.87E-04	2.88E-04	2.87E-04	2.87E-04
CO_2(g) Fugacity	2.02E-06	2.02E-06	2.02E-06	2.02E-06
Solid Phase	**Saturation Index (SI)**			
$Am(OH)_3$(am)	[C]	-1.89	-1.89	-1.89
$Am(OH)_3$(cr-aged)	[C]	-0.59	-0.59	-0.59
$Am(OH)_3$(s)	0.00	0.52	0.52	0.52
$AmOHCO_3$(c)	-0.52	0.00	0.00	0.00

A - The scaled inventory mass of the total emplaced Am(III) at repository closure in 2033 using the 2018-PAIR data (VanSoest, 2018) was used to set the initial Am(III) concentration in Step 1. See APPENDIX A for calculation of the total Am(III).
B - $Am(OH)_3(x)$ x = am, cr-aged, or s.
C - $Am(OH)_3$(am) and $Am(OH)_3$(cr-aged) are not included in DATA0.FM5

The results shown in Tables 4 and 5 are the final equilibrium conditions and concentrations of the modeled system and show the stable solid phase for these conditions. The solid phase with a zero value of its saturation index (SI = 0.0) represents the americium phase which is stable for these final equilibrium chemical conditions.

The purpose of this analysis was to illustrate that the solubility limiting phase at system equilibrium (Step 2) is independent of the phase that was used to set the input Am(III) concentration in Step 1. The reason the phase used to set the input Am(III) concentration was not the stable phase when equilibrium was attained at the end of Step 2 is because the chemical conditions of the reacted brines at equilibrium differ from those of the unreacted brines of Step 1. Indeed, it is not necessary to specify a solubility limiting phase in Step 1 at all, the simulation where the initial Am(III) concentration was input at the inventory values, column 4 in Tables 4 and 5, shows that in Step 2 the EQ6 code finds the most stable phase for the conditions. The results in Tables 4 and 5 show that for the predicted WIPP conditions $AmOHCO_3$(c) is the stable americium bearing phase when $Am(OH)_3$(s) is suppressed, and not the more soluble amorphous and crystalline/aged phases of Neck et al. (2009), this result was supported by the phase-stability diagrams.

Tables 4 and 5 show that the Am(III) solubility slightly decreased on the order of 3E-08 – 8E-08 molal, for ERDA-6 and GWB, under the Neck model. While this small decrease is within the uncertainty of the thermodynamic model it is useful to examine the cause. A shift in the Am(III) species concentrations caused by the change of the Am(III) hydrolysis constants (Table 1) of the Neck model is responsible for the concentration decrease. The largest contributor was the $Am(OH)_2^+$ aqueous species, its concentration decreased by 1E-07 – 2E-07 molal, a decline that was largely offset by increases in the concentrations of other Am(III) aqueous species. The DATA0.FM5 log β value for $Am(OH)_2^+$ aqueous species is 15.7 which is within the uncertainty of the 15.1 ± 0.7 value recommended by Neck et al. (2009), therefore, the slight decrease in the Am(III) concentration is within the model uncertainty.

The EQ3/6 input/output files and the spreadsheet *ERDA6_GWB_Results.xlsx* are archived in the zip file *Neck_An(III)_Model.zip*, which is stored at /nfs/data/CVSLIB/WIPP_EXTERNAL/ap153".

Information Only

Summary and Conclusions

The Neck et. al. (2009) solubility model for the $An^{3+} - Ca^{2+} - Mg^{2+} - Na^{+} - Cl^{-} - H_2O$ system was implemented in the WIPP thermodynamic database DATA0.FM5 creating a new "one off" database DATA0.NK5. Using the EQ3NR code and this new database the An(III) model was compared to the Neck et al. (2009) measured experimental $Nd(OH)_3(s)$ solubility data for both the amorphous and crystalline/aged forms of americium hydroxide. As shown in Figures 1 and 2 of this memo the model response which uses the log K value for the amorphous form provides a good fit to the measured data, while model response for the crystalline aged form reproduces the trend of the data but underestimates the magnitude of the data.

Americium phase-stability diagrams were constructed (Figure 3) based on the thermodynamics of the Am-hydroxide - Am-carbonate system. These diagrams showed that for the chemical conditions (i.e., water activity and $fCO_2(g)$) predicted for the WIPP only $AmOHCO_3(c)$ was the stable form when paired with the amorphous and crystalline forms (am and cr-aged) forms. However, when $AmOHCO_3(c)$ was paired with $Am(OH)_3(s)$ the phase stability diagram showed $Am(OH)_3(s)$ to be the stable phase.

The CRA-2019 DPA baseline solubility model was used to compare the results obtained using the WIPP approved database, DATA0.FM5, and the database updated with the Neck et al. (2009) An(III) model. The results show that Am concentrations and the bulk chemistry of the brines are nearly identical irrespective of the thermodynamic database and initial solubility controlling phase used in Step 1, for both the GWB and ERDA-6. The results also show that if $Am(OH)_3(s)$ is suppressed then $AmOHCO_3(c)$ will be the solubility controlling phase because neither $Am(OH)_3(am)$ or $Am(OH)_3$(cr-aged) are stable for WIPP conditions, thus confirming the findings of the phase-stability diagrams.

The motivation to implement the Neck model and include the amorphous Am-hydroxide phase in the WIPP model can be found in the Wilson et al., (1996) *Conceptual Model Peer Review Report*:

"A second assumption is that actinide precipitates formed in laboratory experiments will allow the crystallinity to mature with time. Since solids are typically less soluble than amorphous precipitates, laboratory solubility studies can then provide an upper concentration limit."

Applying this assumption would be conservative (i.e., higher dissolved actinide concentrations) with respect to actinide concentrations. However, implementation of the Neck et al. (2009) model, which includes the amorphous form of americium hydroxide, and suppressing $Am(OH)_3(s)$ for WIPP recertification work will change the Am(III) solubility controlling phase from an Am-hydroxide phase to a Am-hydroxycarbonate phase, as well as impacting the Am(III) speciation.

Information Only

References

Baes, C. F., and R. E. Mesner. "The hydrolysis of cations John Wiley and Sons Inc." New York (1976).

Choppin, G.R., A.H. Bond, M. Borkowski, M.G. Bronikowski, J.F. Chen, S. Lis, J. Mizera, O. Pokrovsky, N.A. Wall, Y.X. Xia, and R.C. Moore. 2001. Waste Isolation Pilot Plant Actinide Source Term Test Program: Solubility Studies and Development of Modeling Parameters. Albuquerque, NM: Sandia National Laboratories. SAND99-0943. ERMS 518556.

Diakonov, I.I., B. R. Tagirov, K. V. Ragnarsdottir. Standard Thermodynamic Properties and Heat Capacity Equations for Rare Earth Element Hydroxides I . La(OH)3(s) and Nd(OH)3(s). Comparison of Thermochemical and Solubility Data. *Radiochim. Acta* 81, 107 (1998).

Domski, P.S. and C. Sisk-Scott. 2019. "Prediction of Baseline Actinide Solubilities for CRA 2019 with an Updated EQ3/6 Pitzer Thermodynamic Database, DATA0.FM4". Carlsbad, NM: Sandia National Laboratories. ERMS 571178.

Domski, P.S. 2020. DATA0.FM5: Official Release of the Qualified Pitzer Thermodynamic Database, DATA0.FM5, for EQ3/6 under AP-183, Revision 1. Carlsbad, NM: Sandia National Laboratories. ERMS 572791.

Felmy, A.R., D. Rai, and R.W. Fulton. 1990. "The Solubility of AmOHCO3(c) and the Aqueous Thermodynamics of the System Na^+ - Am^{3+} - HCO_3^- CO_3^{2-} - OH^- - H_2O," *Radiochimica Acta*. Vol. 50, 193-204.

Fanghanel, T., J.I. Kim, P. Paviet, R. Klenze and W. Hauser, 1994. Thermodynamics of radioactive trace elements in concentrated electrolyte solutions: Hydrolysis of Cm3+ in NaCl-solutions, Radiochimica Acta, 66/67: 81-87.

Fanghänel, T., and J.I. Kim. 1998. Spectroscopic Evaluation of Thermodynamics of Trivalent Actinides in Brines. Journal of Alloys and Compounds 271–273: 728–737.

Giambalvo, E.R. 2002. Memorandum to L.H. Brush. Subject: Recommended Parameter Values for Modeling An(III) Solubility in WIPP Brines. 25 July 2002. Carlsbad, NM: Sandia National Laboratories. ERMS 522982.

Guillaumont, R., Th. Fanghänel, J. Fuger, I. Grenthe, V. Neck, D. A. Palmer, M. H. Rand (OECD, NEA). Chemical Thermodynamics, Vol. 5, Update on the Chemical Thermodynamics of Uranium, Neptunium, Plutonium, Americium and Technetium, Elsevier, Amsterdam (2003).

Harvie, C.E., N. Møller, and J.H. Weare. 1984. "The Prediction of Mineral Solubilities in Natural Waters: The Na-K-Mg-Ca-H-Cl-SO_4-OH-HCO_3-CO_3-CO_2-H_2O System to High Ionic Strengths at 25 °C," *Geochimica et Cosmochimica Acta*. Vol. 48, no. 4, 723-751.

Neck, V., M. Altmaier, T. Rabung, J. Luetzenkirchen, and T. Fanghänel. 2009. Thermodynamics of Trivalent Actinides and Neodymium in NaCl, $MgCl_2$, and $CaCl_2$ Solutions: Solubility, Hydrolysis, and Ternary Ca-M(III)-OH Complexes. Pure and Applied Chemistry, Vol., 81, no. 9, 1555—1568.

Information Only

Peake, T. 2018. Letter to Mike Brown "2018-12-17 E Letter to CBFO WIPP Issues Summary". U.S. Environmental Protection Agency, Center for Waste Management and Regulations. December 17, 2018

Wilson, C., D. Porter, J. Gibbons, E. Oswald, G. Sjoblom, and F. Caporuscio. 1996. Conceptual Models Supplementary Peer Review Report (December). Carlsbad, NM: Carlsbad Area Office. ERMS 243153.

Information Only

ATTACHMENT A.

WIPP An(III) inventory at closure in 2033 from Tables 5-3 and 5-4 in the 2018-PAIR (Van Soest, 2018) total An(III) inventory (all isotopes of Am, Pu, and Cm) 5.11E+06 Ci, or 6.66E+04 moles.

Scaled for EQ3/6 input:

4.38E-03 mols An(III)/Kg-GWB
4.28E-03 mols An(III)/Kg-ERDA-6

The moles of an element may be approximated from its radioactivity with knowledge of the half-life of the particular isotope and Avogadro's number, via

$$n=[A_{Bq}/N_A][(t_{1/2})/ln2]$$

Where, n = moles; A_{Bq} = radioactivity (Becquerels); N_A = Avogadro's number (atoms/mol); $t_{1/2}$ = half-life (s), and where 1.0 Ci = 3.7E+10 Bq (decays/second).

Information Only